Suppression of the Ablation Phase in Wire Array Z Pinches Using a Tailored Current Prepulse

A. J. Harvey-Thompson,[1] S. V. Lebedev,[1] G. Burdiak,[1] E. M. Waisman,[2] G. N. Hall,[1] F. Suzuki-Vidal,[1] S. N. Bland,[1] J. P. Chittenden,[1] P. De Grouchy,[1] E. Khoory,[1] L. Pickworth,[1] J. Skidmore,[1] and G. Swadling[1]

[1]*Blackett Laboratory, Imperial College, London, SW7 2BW, United Kingdom*

[2]*Sandia National Laboratories, Albuquerque, New Mexico 87185, USA*

(Received 25 March 2011; published 20 May 2011)

A new wire array configuration has been used to create thin shell-like implosions in a cylindrical array. The setup introduces a ~5 kA, ~25 ns current prepulse followed by a ~140 ns current-free interval before the application of the main (~ 1 MA) current pulse. The prepulse volumetrically heats the wires which expand to ~1 mm diameter leaving no dense wire core and without development of instabilities. The main current pulse then ionizes all the array mass resulting in suppression of the ablation phase, an accelerating implosion, and no trailing mass. Rayleigh-Taylor instability growth in the imploding plasma is inferred to be seeded by μm-scale perturbations on the surface of the wires. The absence of wire cores is found to be the critical factor in altering the implosion dynamics.

DOI: 10.1103/PhysRevLett.106.205002 PACS numbers: 52.58.Lq

Fast Z-pinch plasma implosions driven by multi-mega-Ampère currents are very efficient at converting stored electrical energy into x rays. Achieving high x-ray powers by releasing this energy in a short time requires a high degree of azimuthal symmetry of the imploding plasma and a low level of initial axial perturbations seeding the growth of magnetic Rayleigh-Taylor (MRT) instabilities. The highest x-ray powers in Z-pinch implosions were achieved using cylindrical arrays made of large numbers of fine metallic wires (280–300 TW, >2 MJ at ~20% efficiency on the Z facility at SNL [1,2]). Experimental studies of wire array Z pinches have shown [3–5] that even for a large number of wires the arrays do not form a plasma shell imploding as a 2D object. Instead, the wires remain as discrete, compact objects for the first 60%–80% of the implosion and during this time only the coronal plasma, continuously ablated from the stationary cores, are accelerated towards the axis by the $J \times B$ force [4]. This ablation phase determines the initial conditions for the implosion in two ways. First, the ablated plasma fills the interior of the array which contributes to the mitigation of the growth of the MRT instability. Second, the quasiperiodic modulation of the ablation rate along each individual wire occurring at the ''natural'' wavelength (~ 250 μm for W and ~500 μm for Al) is responsible for the large level of axial perturbations at the start of the implosion phase. The existence of the ablation phase is observed in all known wire array Z-pinch experiments (currents between ~1 and 26 MA, and implosion times between ~50 and ~800 ns) and occurs because current is initially carried by the small amount of plasma formed on the wire surfaces, and not by the wire cores themselves.

In this Letter we report on experiments where the ablation phase in wire array Z pinches was suppressed, including dramatic suppression of the axial perturbations in the wires and suppression of the precursor plasma flow. This was achieved by using a short duration low-level current prepulse (~ 25 ns, ~5 kA) followed by a ~140 ns current-free interval before the main (~ 1 MA, 100 ns) current pulse driving the implosion is applied. The energy deposited by the prepulse was sufficient to convert the wires into a gaseous state, and the delay before the main current pulse allowed the wire material to expand uniformly to ~1 mm in diameter. After the start of the main current pulse all wire material becomes ionized. In the absence of core-corona structure the $J \times B$ force is applied to all the array mass which implodes without leaving trailing mass at the initial array diameter. The low amplitude of the MRT instability seen during the early stages of the implosion is consistent with good axial uniformity of the load array. This work suggests that an appropriately shaped current prepulse applied to large wire-number arrays could create the initial conditions for fast Z-pinch implosions approaching the originally sought mass distribution of an axially uniform 2D plasma shell. The critical component of such a prepulse appears to be the presence of a sufficiently long current-free interval before application of the main current.

Experiments were performed on the MAGPIE generator (1.4 MA, 250 ns) and used a setup consisting of two cylindrical wire arrays as shown in Fig. 1. The bottom, inverse wire array acts here as both a generator of the current prepulse for the top, load (imploding) wire array, and also as a fast current switch providing the delay between the prepulse and the main current. It also reduces the rise time of the main current pulse applied to the load array to ~100 ns. Both arrays were made of eight 10–15 μm diameter Al 5056 (5% Mg) wires. The inverse wire array had a diameter of 16 mm and was assembled around an 8 mm diameter cathode rod. The load (imploding) wire array had a diameter of 8 or 17 mm. Heights of the inverse and the load arrays were varied in the range of

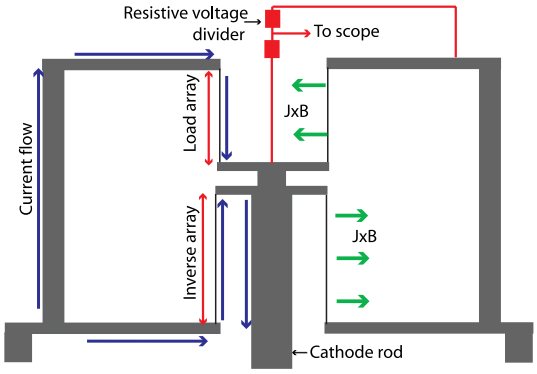

FIG. 1 (color online). Diagram of the array configuration with the resistive voltage divider applied.

20–50 mm and 20–30 mm, respectively. Diagnostics included laser probing (Nd-YAG, 532 nm, 0.4 ns) providing interferometry and schlieren images of the inverse and/or load arrays, gated microchannel plate (MCP) cameras operating in extreme ultraviolet (XUV) (2 ns gate time, imaged radiation ≥ 35 eV), a radial optical streak camera, resistive voltage divider and Rogowski coils. The voltage and dI/dt signals during the prepulse were recorded with a 1 GHz Tektronix scope.

In this setup the total generator current is divided between the inverse and the load array. When the resistance of all wires becomes negligible due to plasma formation, the current division is determined by the mutual inductance and the inductances of the arrays, similar to the current division between the outer and the inner arrays in nested wire arrays [6,7]. For a sufficiently large number of wires in the inverse array the current flowing through the cathode rod will be "returning" to the generator predominantly via the wires of the inverse array and only a few percent of the total current will flow via the load array. The dI/dt signals shown in Fig. 2(a) confirm that between ~20 and 160 ns most of the current is in the inverse array and the current in the load is even below that expected for purely inductive division. At the very beginning of the current pulse, before plasma is formed, the division of current is determined by the resistances of the two arrays. The heating of the inverse array wires and the corresponding increase in their

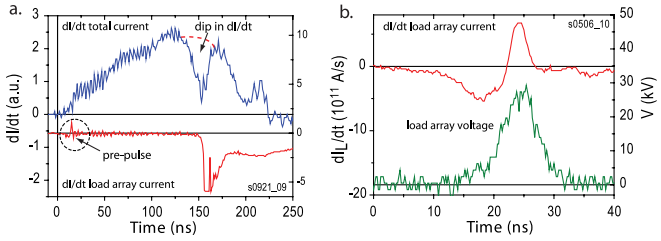

FIG. 2 (color online). Plots of (a) the dI/dt of the total current and the current in just the load array and (b) the dI/dt and the resistive voltage across a 17 mm diameter, 8×15 μm Al load array during the prepulse.

resistance drives a significant fraction of the total current into the load array [Fig. 2(b)], thus generating a current prepulse in the load. The prepulse ends when plasma forms on the wires of the inverse array. The amplitude of the prepulse current can be controlled by varying the relative lengths (and thus resistances) of the load and inverse wire arrays. For equal lengths of the wires in the load and the inverse arrays (27 mm), a ~25 ns long, ~5 kA current prepulse was measured, shown in Fig. 2(b). Figure 2(b) also shows the voltage measured by the resistive voltage probe connected to the bottom of the load array via a 1 mm diameter rod on the array axis as shown in Fig. 1. For such a connection, the measured voltage signal is related to the resistance of the load array wires as the inductive contribution is negligible. Using the measured prepulse load current and voltage in Fig. 2(b), the energy deposited into the load array is ~2 eV/atom. The deposited energy varies slightly from shot to shot (2–3 eV/atom), which could be due to variations in the time of plasma formation in the inverse wire array.

The energy deposited during the prepulse dramatically changes the structure of the load array wires. Figure 3(a) shows an interferogram of an 8 mm diameter, 8×15 μm Al load array obtained 130 ns after the end of the prepulse and before switching of the main current into the load array. The fringes are well defined at all radial positions, and there is no presence of high density wire cores which are always seen in standard wire arrays (see, e.g., [4]). The direction of the fringe shift corresponds to the refractive index being greater than unity, suggesting that the wire material is in the neutral, gaseous state. Using the refractive index for neutral Al ($n = 1 + 6.8 \times 10^{-23}$ cm^3 $\times$ n_{atom} [8]) the measurements of the fringe shift yields the

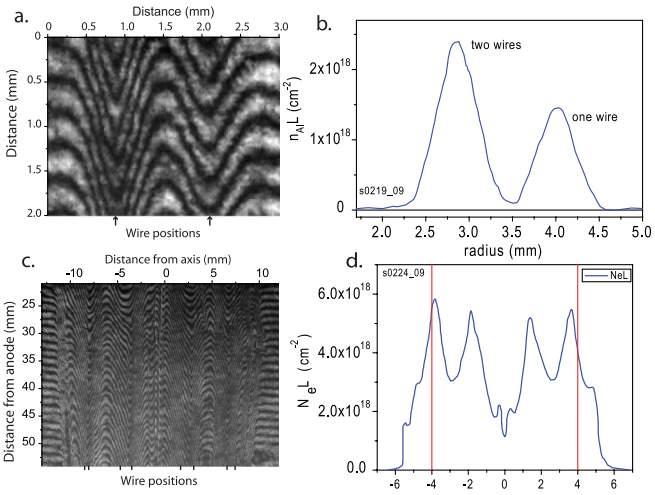

FIG. 3 (color online). (a) Interferogram of a load array taken 2 ns before current switch with the measured Al line density ($n_g L$) shown in (b). (c) Interferogram of a load array obtained $t \sim 40$ ns after current switch with (d) the measured electron line density profile. Red lines indicate initial positions of the wires.

profile of atomic line density $n_{\mathrm{atom}} \times L$ shown in Fig. 3(b). The total number of gaseous atoms (per unit length in axial direction) can be obtained by integrating under this curve, giving $\hat{n}_g = 0.77 \pm 0.1 \times 10^{17}$ cm^{-1} for the edge (single) wire, and $\hat{n}_g = 1.4 \pm 0.1 \times 10^{17}$ cm^{-1} for the two overlapping wires.

Comparison with the total number of atoms in one or two 15 μm diameter wires ($\hat{n} = 1.06 \times 10^{17}$ cm^{-1} and $\hat{n} = 2.12 \times 10^{17}$ cm^{-1}, respectively) suggests that ~70% of total mass has been converted into Al gas. The remaining mass may be in the form of liquid droplets or clusters that are not detected by the interferometer. We also note that if the refractive index calculated for the static electric field polarizability of Al [8] is used ($n = 1 + 4.4 \times 10^{-23}$ cm$^3 \times n_{\mathrm{atom}}$), the measured number of gaseous atoms agrees with total wire mass. Either way, the gaseous state of the expanded wires is consistent with the absence of current in the load array after the end of the current prepulse, which allows the gaseous wires to expand into the surrounding vacuum, free of the $J \times B$ force.

The wires in Figs. 3(a) and 3(b) have expanded to radius of ~0.5 mm in 130 ns after the end of prepulse, which corresponds to an average velocity of 3.8×10^5 cm/s. This allows for an estimate of the initial gas temperature T_g by equating this velocity to $3 \times C_s$, the gas sound speed, giving $T_g \sim 0.45$ eV.

From the end of the current prepulse and until ~140–160 ns (depending on wire diameter used) the generator current remains in the inverse wire array. During this time the wires of the inverse array behave in the same way as wires in standard, imploding wire arrays [9]. The wires remain stationary at their initial positions and ablate plasma which flows radially outwards. Once ~50% of the wire mass is ablated, the inverse array starts to explode, similar to the start of the implosion in standard cylindrical arrays. The start of the explosion phase leads to an increase in the impedance of the current path through the inverse array plasma, and current starts switching into the load array. Laser probing and XUV images show that the explosion phase for the configuration corresponding to current traces shown in Fig. 2(a) starts at ~140 ns, the same time as a dip in the dI/dt of the total current is observed. The subsequent increase in dI/dt at ~160 ns indicates plasma formation in the load array and switching of a significant fraction of the generator current into the load array [Fig. 2(a), bottom trace].

The increase in voltage applied to the expanded load array wires at the start of current switching causes the wires to ionize as can be seen in the interferogram shown in Fig. 3(c) obtained ~40 ns after current switch. The direction of the fringe shift now corresponds to the refractive index being below unity, consistent with wire material being in a plasma state. The wires have expanded further to ~2 mm diameter, presumably due to an increase in temperature, while the $J \times B$ force is insufficient to oppose expansion up to this time. The profile of the electron line density, $n_e L$, calculated from the fringe shifts measured in Fig. 3(c) is shown in Fig. 3(d). The total (per unit length in the axial direction) number of electrons in the array (N_e) can be obtained by integrating the profile of $n_e L$. The measured total number of electrons $N_e = (3.8 \pm 0.2) \times 10^{18}$ cm^{-1} is ~4 times larger than the total number of atoms in all eight wires of this array (8.46×10^{17} cm^{-1}), suggesting that all array mass is ionized to an average charge of $Z \sim 4$. The interferogram does not show any evidence of dense wire cores and, together with schlieren images, shows a high degree of axial uniformity and an absence of quasiperiodic density perturbations on a "natural" wavelength which are always present in standard wire arrays [4].

The sharp radial density gradients seen on the interferogram [Fig. 3(c)] at the edges of the wire array suggest that the array material is starting to accelerate towards the axis and the $J \times B$ force appears to be greatest at the outer edges of the gaseous wires. The ratio of interwire gap to wire radius, $\pi R_0/NR_w$, for 8 and 17 mm diameter arrays at this time is ~1.5 and ~3, respectively. It has been theoretically found that for ratios comparable or smaller than ~3 that current is concentrated at the sides of the wire furthest from the array axis [6,10].

The implosion dynamics of the load array was measured using radial optical streak images. A typical radial streak image of an implosion of a 17 mm diameter, 8×10 μm Al wire array is shown in Fig. 4(a). It is seen that emission from the wires starts at ~140 ns, at the time when the current is just starting to switch into the load, and the size of the emitting region is similar to the diameter of the expanded wires measured with interferometry. No emitting precursor is seen on the array axis suggesting little (if any) ablation occurs. The implosion of the array is very rapid, with an implosion time of ~80 ns. The implosion proceeds with a continuously increasing velocity which is consistent with the absence of resistive wire cores and little plasma prefill, allowing the $J \times B$ force to act upon all the array mass. The measured implosion trajectory is consistent with a thin shell-like implosion driven by a linearly

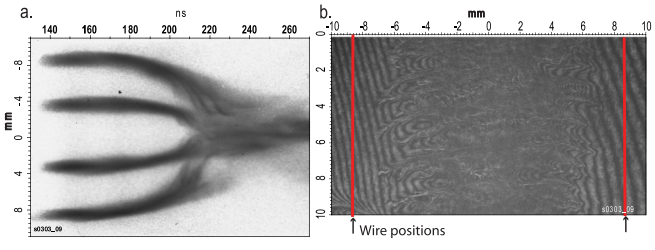

FIG. 4 (color online). (a) Radial optical streak photograph showing implosion of a 17 mm diameter, 8×10 μm Al load array. (b) Interferogram of a load array taken 76 ns after current switch showing no trailing mass between the original wire positions (red lines) and the imploding plasma.

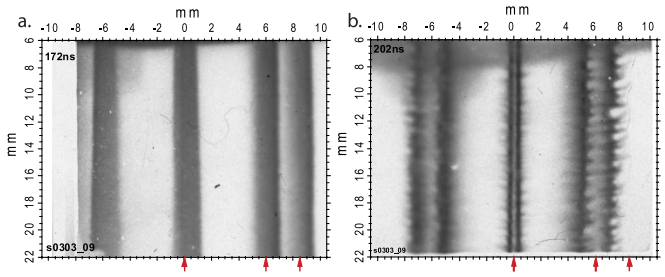

FIG. 5 (color online). (a),(b) XUV images showing development of MRT instability during implosion of the load array. Arrows show initial positions of the wires.

rising current reaching 1.4 MA (maximum generator current) in ~95 ns. Obtaining direct measurements of the load current will be a priority for future experiments.

The initial participation of all array mass in the implosion is also confirmed by the interferogram presented in Fig. 4(b), which shows no measurable fringe shift in the region between the original wire locations (radius 8.5 mm) and a radius of ~6 mm (< 0.1 fringe, corresponding to an electron line density of $n_e l < 4 \times 10^{16}$ cm^{-2}). Multiplying this electron line density by the width of the region (2×2.5 mm) yields an upper limit on the mass in this region of ~0.5%–2% of the array mass (assuming Z = 4 or Z = 1, respectively). This is in contrast to implosions of standard wire arrays, where a significant fraction of the array mass remains at the initial array radius [4,11].

The interferogram in Fig. 4(b) also shows that for radii smaller than ~6 mm there is a considerable amount of plasma even close to the implosion time. This trailing mass is due to the development of the MRT instability growing during the implosion. The growth of the MRT instability is illustrated by XUV images shown in Fig. 5, which were obtained in the same shot at times 30 and 60 ns after the current switch. The first image shows wires expanded to a diameter of ~2 mm which are still at their original positions. The stronger emission seen at the outer edges of the array is consistent with the larger current density there as was discussed above. No detectable axial perturbations are seen in the emission intensity or shape of the wires. The second image clearly shows that by this time the wires moved inwards by $\Delta r \sim 1.5$ mm, and a well-developed MRT instability is now seen. The wavelength of the instability, averaged over the full length of the wires, is equal to 0.8 ± 0.2 mm, and the amplitude of the perturbations is estimated to be ~0.4 mm.

The observed amplitude of the instability can be used to estimate the characteristic level of initial perturbations on the wires at the start of the implosion. For MRT instabilities in cylindrical geometry, analytical solutions ([12], and references therein) show that the amplitude grows as $\xi = \xi_0 \exp(G(t))$, where $G(t) = \int(\gamma(\tau)d\tau)$, $\gamma = \sqrt{a \times k}$, a is the acceleration, and k is the wave number of the instability. It is well known (see, e.g., discussion in Ref. [12], p. 193) that the function G has a universal dependence on the instantaneous radial convergence (r/R_0) of the imploding shell, and for small displacements $G/\sqrt{kR_0} = \sqrt{(1 - r/R_0)} \times F$, where the form factor $F \sim 1.63$–1.83 only slightly depends on the temporal shape of the current driving the implosion. Using measurements from Fig. 5(b), $\Delta r/R_0 = 0.17$, $\lambda = 0.8$ mm and $\xi = 0.4$ mm, we can estimate the number of e foldings of the MRT growth as $G = 5.56$–6.22 and the corresponding amplitude of initial perturbations as $\xi_0 = 1.5 - 0.8$ μm. This estimate suggests that the tailored current prepulse produces a low level of initial perturbations on the individual wires.

The high x-ray powers obtained in standard arrays are partly a consequence of the limited growth of MRT instabilities during the snowplow implosion phase. Instabilities develop faster in accelerating thin shell-like implosions; however, there are no large scale initial perturbations to seed that growth due to the suppressed ablation. Techniques suggested to reduce MRT growth in plasma shell implosions can now be tested in this geometry. The limited ablation also reduces the mass that arrives at the array axis before the main implosion. It is thought this may lead to an increase in shock heating at the point of implosion and increased x-ray powers [13]. Finally, the absence of trailing mass should allow more current to be coupled to the pinch at stagnation increasing the energy of the associated x-ray pulse.

The authors are grateful to Dr. M. E. Cuneo and Dr. R. B. Spielman for many useful discussions. This research was sponsored by Sandia National Laboratories Albuquerque and the NNSA under DOE Cooperative Agreement No. DE-F03-02NA00057.

[1] C. Deeney *et al.*, Phys. Rev. Lett. **81**, 4883 (1998).
[2] M. Jones *et al.*, APS Meeting Abstracts, 2010 (unpublished), p. 5010.
[3] C. Deeney *et al.*, Phys. Rev. E **56**, 5945 (1997).
[4] S. V. Lebedev *et al.*, Phys. Plasmas **8**, 3734 (2001).
[5] M. E. Cuneo *et al.*, Phys. Rev. E **71**, 046406 (2005).
[6] A. L. Velikovich *et al.*, Phys. Plasmas **9**, 1366 (2002).
[7] S. N. Bland *et al.*, Phys. Plasmas **10**, 1100 (2003).
[8] G. S. Sarkisov *et al.*, Phys. Rev. A **73**, 042501 (2006).
[9] A. J. Harvey-Thompson *et al.*, Phys. Plasmas **16**, 022701 (2009).
[10] E. M. Waisman, J. Appl. Phys. **50**, 23 (1979).
[11] V. V. Alexandrov *et al.*, Sov. J. Exp. Theor. Phys. **97**, 745 (2003).
[12] D. D. Ryutov *et al.*, Rev. Mod. Phys. **72**, 167 (2000).
[13] R. W. Lemke *et al.*, Phys. Rev. Lett. **102**, 025005 (2009).